Transient Thermal Response Due to Periodic Heating on a Convectively Cooled Substrate

Timothy S. Fisher, C. Thomas Avedisian, and J. Peter Krusius, *Senior Member, IEEE*

Abstract— **The increasing use of highly integrated circuits in portable electronics, which may operate for relatively short periods of time, has opened the possibility of utilizing heat storage to maintain device temperatures below reliability limits. The present study considers a strategy in which the power dissipation of a device is periodically reduced and increased in order to decrease its peak temperature. A two-dimensional, axisymmetric, chip-on-substrate geometry is assumed with convective cooling on the bottom side. Exact solutions for the steady-periodic and complete transient responses are presented. Peak temperature rise is shown to depend on several geometric, thermal, and electrical parameters. The results indicate that thermal resistance can be minimized with an appropriate choice of substrate thickness. Also, cycle periods of tens of seconds can be achieved for typical electronic packages while retaining the benefits of periodic heating.**

Index Terms— **Transient heat conduction, electronic cooling, periodic heating.**

Nomenclature

a	Heat-source radius, m, see Fig. 2.
b	Substrate radius, m, see Fig. 2.
b^*	Nondimensional substrate radius, b/a.
Bi	Biot number, ha/k.
Fo	Periodic Fourier number, $\alpha p/a^2$.
h	Heat transfer coefficient, W/m^{2}K.
k	Substrate thermal conductivity, W/mK.
l	Substrate thickness, m, see Fig. 2.
l^*	Nondimensional substrate thickness, l/a.
p	Cycle period, s, see Fig. 1.
q''	Heat flow per unit area, W/m^2.
r, z	Cylindrical coordinates, m.
t	Time, s.
T	Temperature, K.
α	Substrate thermal diffusivity, m^2/s.
β	Power ratio, $q''_{\min}/q''_{\max}$, see Fig. 1.
Φ	Nondimensional temperature rise at heated surface, see (11).
θ^*	Nondimensional temperature rise, $(T-T_\infty)h/q''_{\max}$.
ξ	Duty cycle, t_1/p, see Fig. 1.

Manuscript received June 1, 1995; revised October 31, 1995. This work was supported by the Semiconductor Research Corporation (SRC) and the Industry-Cornell University Alliance for Electronic Packaging. T. S. Fisher was supported by a graduate fellowship from the SRC.

T. S. Fisher and C. T. Avedisian are with the Sibley School of Mechanical and Aerospace Engineering, Cornell University, Ithaca, NY 14853 USA.

J. P. Krusius is with the School of Electrical Engineering, Cornell University, Ithaca, NY 14853 USA.

Publisher Item Identifier S 1070-9894(96)01351-5.

I. Introduction

The breadth of applications for microelectronics has increased greatly in recent years. At the same time, volumetric heat generation rates from electronic modules have risen dramatically and are projected to continue a rapid rate of increase [1]. Most cooling designs for electronic systems are based on steady-state operation with the assumption that the power dissipation remains constant in time. However, peak application workloads may vary from milliseconds to tens of seconds. Such variability suggests that the heat storage capacity of packaging materials may be used to enhance conventional cooling in electronic systems, particularly for compact, single-user systems. Heat capacity can be exploited by temporal power management, which may be achieved, for example, by regulating on-chip functions or by dynamic variation of the system's clock frequency [2]. The effects of transient heating on chip temperatures are examined in this paper using a simple thermal model: a single chip with a time-dependent power dissipation on a convectively cooled substrate.

The steady-state and transient characteristics of the common chip-on-substrate geometry with convective cooling have been considered in many previous studies. An axisymmetric geometry has been shown to accurately depict the heat transfer characteristics of a three-dimensional Cartesian geometry under steady-state conditions [3], [4], and a highly accurate approximate solution has been established [5]. Resistance–capacitance (R–C) networks have been used to study the transient characteristic of common electronic packages [6]–[9]. Transient experimental results have also been obtained for several types of heat flux profiles: step, single pulse [9], and periodic pulses [10]. Exact solutions for the transient response have also been presented in [11] and [12]. In general, the foregoing studies have consistently predicted and measured package-level thermal time constants of the order of minutes.

The relatively large thermal time constants of many electronic modules may be exploited to allow higher power dissipation during the startup transient. A schematic of a possible heat-flux waveform and the resulting temperature profile appears in Fig. 1. In the figure, a heat flux, $q''_{\max}$, is applied at $t=0$ and persists until $t=t_0$, the time when the chip temperature equals its maximum, $T_{\max}$. The initial transient allows full power to be applied without exceeding the maximum allowable chip temperature. For times greater than t_0, heat flux is periodically reduced and increased in order to maintain the maximum chip temperature below $T_{\max}$. For later reference, we define the duty cycle as the fraction of a cycle

1070–9894/96$05.00 © 1996 IEEE

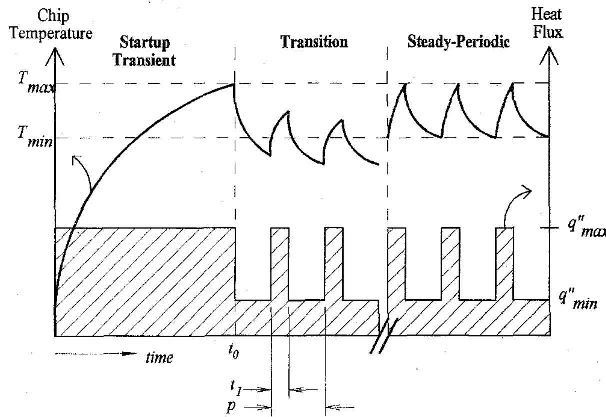

Fig. 1. Sketch of the heat-flux waveform and resulting temperature profile for a time-dependent heat source.

period spent at peak power, $\xi = t_1/p$, and the power ratio as the ratio of minimum to maximum heat flux, $\beta = q''_{\text{min}}/q''_{\text{max}}$.

From the foregoing discussion, it appears that the periodic heating concept may be useful for electronic applications. The thermal benefits of periodic heating have been intimated in prior work, but a systematic study of the thermal characteristics of periodic heating has not yet been published. The present paper uses exact, infinite-series solutions to the heat diffusion equation to provide insights into thermal performance for the case of periodic heating on an axisymmetric substrate. A representative test case is presented, and the influence of several parameters is studied in order to identify the conditions best-suited for periodic heating.

II. Theory and Analysis

The problem geometry, shown in Fig. 2, consists of a circular heat source of radius a producing a uniform, time-dependent heat flux, $q''(t)$, and centered on a circular-cylindrical substrate of radius b and thickness l. The top and side surfaces are adiabatic, while the bottom surface is convectively cooled with a constant and uniform heat transfer coefficient, h. The assumption of a constant and uniform heat transfer coefficient may not be precisely satisfied under certain conditions, such as natural and mixed convection. We note, however, that average heat transfer coefficients are found to be sufficiently accurate for many engineering applications.

In studying general configurations, it becomes convenient to use a nondimensional form. The independent parameters of the problem may be normalized by using the heat source radius, a, as a reference length

$$\begin{aligned} \theta^* &= \frac{(T - T_\infty)h}{q''_{\text{max}}} \\ r^* &= \frac{r}{a} \\ b^* &= \frac{b}{a} \\ z^* &= \frac{z}{a} \\ l^* &= \frac{l}{a} \end{aligned}$$

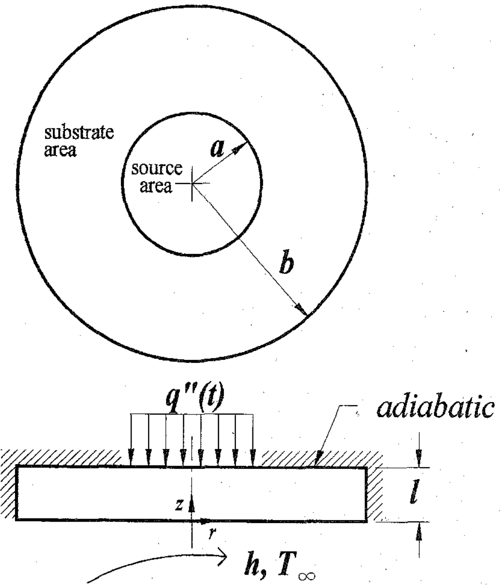

Fig. 2. Axisymmetric source-on-substrate geometry.

$$\begin{aligned} Bi &= \frac{ha}{k} \\ Fo &= \frac{\alpha p}{a^2} \\ \tau &= \frac{t}{p}. \end{aligned} \tag{1}$$

In the above equation, θ^* is a nondimensional temperature rise above ambient with q''_{max}/h as its reference temperature, Bi represents the Biot number, Fo is a periodic Fourier number, a measure of the ratio between the heat-flux waveform's period and the thermal conduction time constant of the system. The variable τ represents the number of elapsed cycle periods.

Assuming time scales greater than 10^{-6} s, large enough to neglect hyperbolic effects for most applications in microelectronics [13], the standard heat diffusion equation can be written in nondimensional form as

$$\frac{1}{Fo}\frac{\partial \theta^*}{\partial \tau} = \frac{1}{r^*}\frac{\partial}{\partial r^*}\left(r^*\frac{\partial \theta^*}{\partial r^*}\right) + \frac{\partial^2 \theta^*}{\partial z^{*2}}. \tag{2}$$

In terms of nondimensional quantities, the boundary conditions for the present problem are

$$\begin{aligned} &\left.\frac{\partial \theta^*}{\partial r^*}\right|_{r^*=0} = 0 \\ &\left.\frac{\partial \theta^*}{\partial r^*}\right|_{r^*=b^*} = 0 \\ &\left.\frac{\partial \theta^*}{\partial z^*}\right|_{z^*=0} = Bi\theta^*(r^*, 0, \tau) \\ &\left.\frac{\partial \theta^*}{\partial z^*}\right|_{z^*=l^*} = \begin{cases} Bi\left[\dfrac{q''(\tau)}{q''_{\text{max}}}\right] & 0 \le r^* \le 1 \\ 0 & 1 \le r^* \le b^* \end{cases}. \end{aligned} \tag{3}$$

The need for an initial condition depends on the information desired. For the complete transient response, the initial condition must be specified, but for the steady-periodic solution, an initial condition is unnecessary.

The complete transient response can be obtained through the use of Duhamel's method [14], which utilizes the temperature response due to a sudden application of constant, uniform heat flux. The single-step solution appears in [12] for the initial condition $\theta^*(r^*, z^*, 0) = 0$

$$\theta_A^*(r^*, z^*, \tau) = \frac{1+Bi\cdot z^*}{b^{*2}} + \frac{2Bi}{b^{*2}}\sum_{m=1}^{\infty}\left\{\frac{J_1(\lambda_m)J_0(\lambda_m r^*)}{\lambda_m^2 J_0^2(\lambda_m b^*)} \cdot \frac{\cosh(\lambda_m z^*) + \frac{Bi}{\lambda_m}\sinh(\lambda_m z^*)}{\sinh(\lambda_m l^*) + \frac{Bi}{\lambda_m}\cosh(\lambda_m l^*)}\right\} - \frac{2Bi\cdot l^*}{b^{*2}}\sum_{n=1}^{\infty}\left\{\frac{\cos(\mu_n l^*) + \frac{Bi}{\mu_n}\sin(\mu_n l^*)}{(\mu_n l^*)^2 + Bi\cdot l^*(1+Bi\cdot l^*)} \cdot \left[\cos(\mu_n z^*) + \frac{Bi}{\mu_n}\sin(\mu_n z^*)\right]e^{-\mu_n^2 Fo\cdot\tau} \cdot \left[1 + 2\sum_{p=1}^{\infty}\frac{\mu_n^2}{\lambda_p(\lambda_p^2+\mu_n^2)}\frac{J_1(\lambda_p)J_0(\lambda_p r^*)}{J_0^2(\lambda_p b^*)}e^{-\lambda_p^2 Fo\cdot\tau}\right]\right\} \tag{4}$$

where $J_m(\cdot)$ are Bessel functions of the first kind and order m, λ_i are roots of $J_1(\lambda_i b^*) = 0$, and μ_n are roots of $\mu_n \tan(\mu_n l^*) = Bi$. The Duhamel solution proceeds by summing contributions from sequential applications of heat flux (see Fig. 1)

$$\theta_D^*(r^*, z^*, \tau) = \theta_A^*(r^*, z^*, \tau) + \sum_{q=1}^{n}(-1)^q(1-\beta) \cdot \theta_A^*(r^*, z^*, \tau - s_q) \tag{5}$$

where

$$s_q = \begin{cases} \tau_0 + \frac{q-1}{2} & q \text{ odd} \\ \tau_0 + \frac{q-2}{2} + (1-\xi) & q \text{ even} \end{cases},$$

and

$$n = \text{number of changes in heat flux after } \tau = 0.$$

In general, many terms in the series of (5) must be evaluated before the steady-periodic regime is reached.

When only steady-periodic results are desired, the method of complex temperature is most efficient. To obtain a complex temperature solution, the periodic heat flux must be converted to a Fourier series

$$\frac{q''(\tau)}{q''_{\max}} = (\xi - \xi\beta + \beta) + \frac{1-\beta}{\pi}\sum_{n=1}^{\infty}\cdot\left[\frac{\sin(2\pi n\xi)}{n}\cos(2\pi n\tau) + \frac{1-\cos(2\pi n\xi)}{n}\sin(2\pi n\tau)\right]. \tag{6}$$

The first term on the right-hand side of (6) is independent of time. Thus, superposition can be invoked to divide the solution, θ_C^*, into steady and transient components

$$\theta_C^*(r^*, z^*, \tau) = \theta_S^*(r^*, z^*) + \theta_T^*(r^*, z^*, \tau). \tag{7}$$

The solution for $\theta_S^*(r^*, z^*)$ can be obtained in a straightforward manner by separation of variables [12].

The solution for the transient component, $\theta_T^*(r^*, z^*, \tau)$, can be obtained by the method of complex temperature, which requires the construction of a supplementary problem with real and imaginary components. Details of the method can be found in [14]. The method suggests a time-varying solution of the form

$$\theta_T^*(r^*, z^*, \tau) = \sum_{n=1}^{\infty}\{\text{Re}\,[\vartheta_n(r^*, z^*)e^{i2\pi n\tau}] + \text{Im}\,[\zeta_n(r^*, z^*)e^{i2\pi n\tau}]\}. \tag{8}$$

Both the real and imaginary terms in (8) must satisfy the governing equation (2) and the homogeneous boundary conditions in (3). For the heat flux boundary condition ($z^* = l^*$, $0 \le r^* \le 1$), the terms are subject to the following, which are based on the Fourier series terms in (6)

$$\frac{\partial}{\partial z^*}\left\{\sum_{n=1}^{\infty}[\vartheta_n(r^*, z^*)e^{i2\pi n\tau}]\right\}\Bigg|_{z^*=l^*} = \frac{Bi(1-\beta)}{\pi}\sum_{n=1}^{\infty}\left[\frac{\sin(2\pi n\xi)}{n}e^{i2\pi n\tau}\right] \tag{9a}$$

$$\frac{\partial}{\partial z^*}\left\{\sum_{n=1}^{\infty}[\zeta_n(r^*, z^*)e^{i2\pi n\tau}]\right\}\Bigg|_{z^*=l^*} = \frac{Bi(1-\beta)}{\pi}\sum_{n=1}^{\infty}\left[\frac{1-\cos(2\pi n\xi)}{n}e^{i2\pi n\tau}\right]. \tag{9b}$$

ϑ_n and ζ_n can be solved by separation of variables, and the final expression for θ_T^* becomes

$$\theta_T^*(r^*, z^*, \tau) = \frac{Bi(1-\beta)}{\pi b^{*2}}\sum_{n=1}^{\infty} \cdot\left\{\text{Re}\left[\frac{\sin(2\pi n\xi)}{n\delta_n}\left[\frac{\frac{\delta_n}{Bi} + \tanh(\delta_n z^*)}{1 + \frac{\delta_n}{Bi}\tanh(\delta_n l^*)}\right] \cdot \frac{\cosh(\delta_n z^*)}{\cosh(\delta_n l^*)}e^{i2\pi n\tau}\right] + \text{Im}\left[\frac{1-\cos(2\pi n\xi)}{n\delta_n}\left[\frac{\frac{\delta_n}{Bi} + \tanh(\delta_n z^*)}{1 + \frac{\delta_n}{Bi}\tanh(\delta_n l^*)}\right] \cdot \frac{\cosh(\delta_n z^*)}{\cosh(\delta_n l^*)}e^{i2\pi n\tau}\right]\right.$$

$$+2\sum_{m=1}^{\infty}\left\{\mathrm{Re}\left[\frac{\sin(2\pi n\xi)}{n\lambda_m\gamma_{mn}}\left[\frac{\frac{\gamma_{mn}}{Bi}+\tanh(\gamma_{mn}z^*)}{1+\frac{\gamma_{mn}}{Bi}\tanh(\gamma_{mn}l^*)}\right]\cdot\frac{\cosh(\gamma_{mn}z^*)}{\cosh(\gamma_{mn}l^*)}\frac{J_0(\lambda_m r^*)J_1(\lambda_m)}{J_0^2(\lambda_m b^*)}e^{i2\pi n\tau}\right]+\mathrm{Im}\left[\frac{1-\cos(2\pi n\xi)}{n\lambda_m\gamma_{mn}}\left[\frac{\frac{\gamma_{mn}}{Bi}+\tanh(\gamma_{mn}z^*)}{1+\frac{\gamma_{mn}}{Bi}\tanh(\gamma_{mn}l^*)}\right]\cdot\frac{\cosh(\gamma_{mn}z^*)}{\cosh(\gamma_{mn}l^*)}\frac{J_0(\lambda_m r^*)J_1(\lambda_m)}{J_0^2(\lambda_m b^*)}e^{i2\pi n\tau}\right]\right\}\Bigg\} \quad (10)$$

where $\delta_n \equiv [i2\pi n/Fo]^{1/2}$; λ_m are roots of $J_1(\lambda_m b^*) = 0$; $\gamma_{mn} \equiv [\delta_{n^2} + \lambda_{m^2}]^{1/2}$. The final expression for $\theta_C^*(r^*, z^*, \tau)$ can be obtained by summing the steady-state term (θ_S^* from [12]) and (10).

The critical thermal parameter in electronic packaging problems is usually the maximum heat-source temperature, which is typically constrained to 100°C or lower. Neglecting the internal heat-source resistance, this maximum will occur along the axis of symmetry at the top of the substrate (i.e., at $r^* = 0$, $z^* = l^*$). A nondimensional temperature rise at the foregoing spatial location is defined as

$$\Phi = \theta^*(0, l^*, \tau). \quad (11)$$

In the above equation, either the Duhamel solution, $\theta_D^*(0, l^*, \tau)$ from (5), or the complex temperature solution, $\theta_C^*(0, l^*, \tau)$ from (6), may be used. The complex temperature solution takes the form

$$\Phi = \frac{\xi-\xi\beta+\beta}{b^{*2}}\left[(Bi\cdot l^*+1)+2Bi\sum_{n=1}^{\infty}\cdot\left[\frac{J_1(\lambda_n)}{\lambda_n^2 J_0^2(\lambda_n b^*)}\left(\frac{\frac{\lambda_n}{Bi}+\tanh(\lambda_n l^*)}{1+\frac{\lambda_n}{Bi}\tanh(\lambda_n l^*)}\right)\right]\right]$$
$$+\frac{Bi(1-\beta)}{\pi b^{*2}}\sum_{n=1}^{\infty}\cdot\left\{\mathrm{Re}\left[\frac{\sin(2\pi n\xi)}{n\delta_n}\left[\frac{\frac{\delta_n}{Bi}+\tanh(\delta_n l^*)}{1+\frac{\delta_n}{Bi}\tanh(\delta_n l^*)}\right]e^{2\pi in\tau}\right]+\mathrm{Im}\left[\frac{1-\cos(2\pi n\xi)}{n\delta_n}\left[\frac{\frac{\delta_n}{Bi}+\tanh(\delta_n l^*)}{1+\frac{\delta_n}{Bi}\tanh(\delta_n l^*)}\right]e^{2\pi in\tau}\right]\right.$$
$$\left.+2\sum_{m=1}^{\infty}\left\{\mathrm{Re}\left[\frac{\sin(2\pi n\xi)}{n\lambda_m\gamma_{mn}}\left[\frac{\frac{\gamma_{mn}}{Bi}+\tanh(\gamma_{mn}l^*)}{1+\frac{\gamma_{mn}}{Bi}\tanh(\gamma_{mn}l^*)}\right]\cdot\frac{J_1(\lambda_m)}{J_0^2(\lambda_m b^*)}e^{2\pi in\tau}\right]+\mathrm{Im}\left[\frac{1-\cos(2\pi n\xi)}{n\lambda_m\gamma_{mn}}\left[\frac{\frac{\gamma_{mn}}{Bi}+\tanh(\gamma_{mn}l^*)}{1+\frac{\gamma_{mn}}{Bi}\tanh(\gamma_{mn}l^*)}\right]\cdot\frac{J_1(\lambda_m)}{J_0^2(\lambda_m b^*)}e^{2\pi in\tau}\right]\right\}\right\}. \quad (12)$$

The nondimensional temperature rise, Φ, depends on seven parameters: τ, l^*, b^*, Bi, Fo, ξ, and β. The influence of several of these parameters on thermal enhancement from periodic heating is considered in the following section.

III. Analytical Results

In order to elucidate the theoretical development of the previous section, the complete transient profile for a specific case is now presented. The assumed properties of the substrate are as follows: $a = 1\times10^{-2}$ m, $l = 5\times10^{-3}$ m, $b = 2.5\times10^{-2}$ m, $k = 10$ W/mK, $\alpha = 1\times10^{-5}$ m^2/s. The foregoing values are representative of a generic ceramic substrate with moderate thermal conductivity. Forced air convection is assumed, with a heat transfer coefficient, $h = 100$ W/m^{2}K. The cycle period, p, is taken as 1 second. With the duration of maximum heat flux and the power ratio taken as 0.5 s and 0.25, respectively, the nondimensional parameters for the present example become: $l^* = 0.5$, $b^* = 2.5$, $Bi = 0.1$, $Fo = 0.1$, $\xi = 0.5$, and $\beta = 0.25$.

The resulting nondimensional temperature as a function of time appears in Fig. 3 for several different heating profiles. The top curve represents the response due to a constant heat source and exhibits an exponential-like form. The bottom curve corresponds to the temperature response due to a periodic, square-wave heat flux without an initial startup pulse. In this entirely periodic mode, the temperature oscillates about an exponential-like mean profile, with local temperature minima and maxima occurring at the beginning and end, respectively, of the application of peak heat flux. The middle curve corresponds to the temperature response due to a heat flux profile of the type shown in Fig. 1.

The middle curve of Fig. 3 follows the top curve exactly until periodic heating commences at $\tau_0 = 32.5$ (or $t_0 = 32.5$ s), when the temperature approximately equals the maximum steady-periodic temperature. Immediately following the initiation of periodic heating, the middle curve exhibits a decreasing trend for approximately ten cycle periods and then proceeds to increase toward its steady-periodic profile.

The local minimum in average temperature exhibited by the middle curve of Fig. 3 occurs only under certain circumstances. For instance, it can be shown that the minimum does not occur under a lumped capacitance approximation (i.e., uniform substrate temperature). To determine the presence or absence of a local minimum, an average temperature rise, based on an average heat flux $q''_{\text{ave}} = q''_{\max}(\xi-\xi\beta+\beta)$ over one

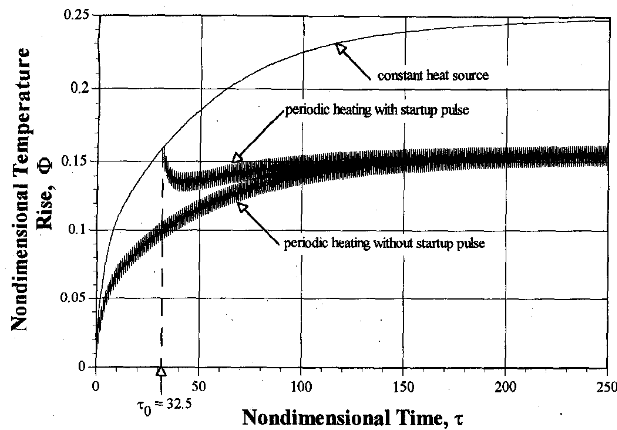

Fig. 3. Nondimensional temperature rise, Φ, as a function of time, τ, for constant heating and periodic heating with and without a startup pulse.

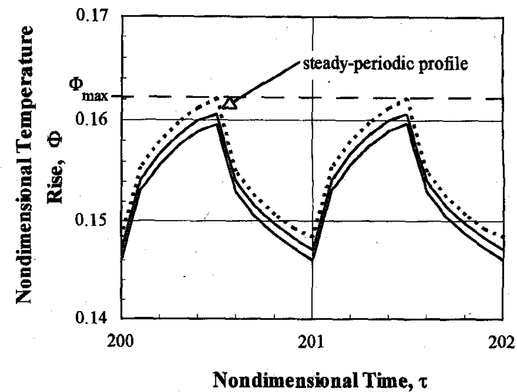

Fig. 5. Nondimensional temperature rise, Φ, as a function of time, τ. Steady-periodic regime.

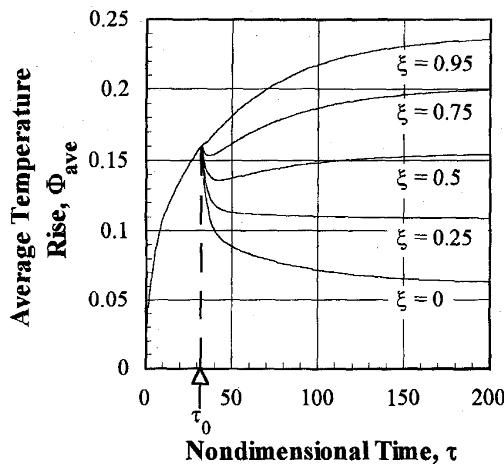

Fig. 4. Average temperature rise, Φ_{ave}, as a function of time, τ, and duty cycle, ξ.

cycle ($\Delta\tau = 1$), is computed for a heat flux profile of the type shown in Fig. 1. The time variation of average temperature for duty cycles ranging from 0–0.95 appears in Fig. 4. All other conditions are the same as those for Fig. 3.

After time $\tau_0 = 32.5$ in Fig. 4, periodic heating commences, and the average heat flux decreases. Just after τ_0, the effect of this reduction is confined to the substrate region near the heated surface due to finite thermal penetration caused by conductive resistance. As a result, the temperature, and consequently the heat rejection, at the convective surface remains relatively high. If the average heat input is less than the heat rejected, the internal energy, and thus the average temperature, will decrease as illustrated by curves in Fig. 4 for duty cycles $\xi = 0, 0.25, 0.5, \text{and} 0.75$. Conversely, if the average heat input remains larger than the heat rejected, the average temperature will continue to rise, as it does for $\xi = 0.95$.

With increasing time beyond τ_0 in Fig. 4, the effect of the reduced heat input penetrates through the substrate to the convective surface, and the convective heat transfer moderates. If this moderated heat removal is less than the average heat input, an increase in average temperature will occur as shown in Fig. 4 for the largest duty cycles $\xi = 0.5, 0.75, \text{and} 0.95$. For small duty cycles (and thus small average heat fluxes), the heat input remains less than the heat rejected, and the average temperature decreases asymptotically after τ_0 to a steady-state value. A local minimum, exhibited by a temperature reduction just after τ_0 followed by a temperature increase, is observed for only two of the duty cycles, $\xi = 0.5$ and 0.75, in Fig. 4. Research is ongoing to determine the precise conditions under which the local minimum occurs.

Figure 5 magnifies the middle and bottom curves of Fig. 3 after 200 cycle periods. The steady-periodic temperature profile, computed from (12), is shown with a dotted line. In the figure, the curves that represent the complete transient solution (solid lines) are seen to approach the steady-periodic profile to within 2% after 200 cycles. The maximum temperature rise, hereafter denoted by Φ_{max}, occurs at the end of the application of peak heat flux and corresponds to $\tau = \xi$ in the steady-periodic solution of (12).

The maximum temperature rise, Φ_{max}, is critically important in the design of microelectronics and will be used in the following paragraphs to characterize the effects of periodic heating as relevant physical parameters are varied. The set of values shown in Table I serves as a reference for the parameters held constant, unless otherwise noted, in subsequent figures.

Temperature can be minimized with an appropriate choice of substrate thickness under steady-state conditions, as demonstrated in [4]. The minimization also occurs when the source is periodically pulsed, as shown in Fig. 6. In the figure, curves of different duty cycles, ξ, converge to $\Phi_{max} = 1$ for very small substrate thicknesses. This convergence reflects the lack of extensive heat capacity of very thin substrates. As the substrate thickness increases, a clear minimum temperature rise is observed for $l^* \sim 1$ for all duty cycles. As the substrate thickness increases further, axial conductive resistance dominates, causing an increase in the nondimensional temperature rise. The minimum is the result of a compromise between heat spreading and axial thermal resistance for the steady-state case

TABLE I
DEFAULT VALUES OF VARIABLE PARAMETERS

l^*	0.5
b^*	2.5
Bi	0.1
Fo	0.1
ξ	0.25
β	0.0

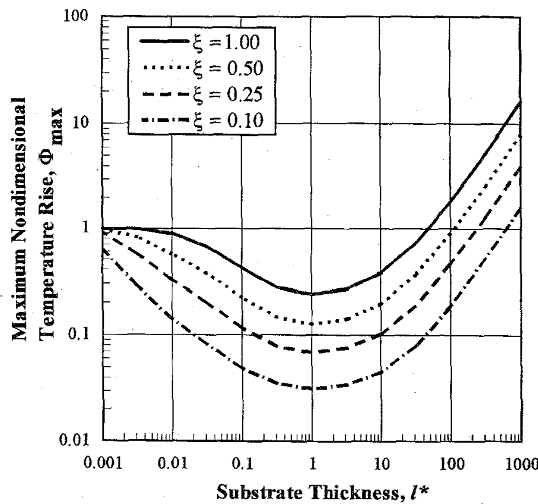

Fig. 6. Maximum nondimensional temperature rise, $\Phi_{\max}$, as a function of substrate thickness, l^*, and duty cycle, ξ.

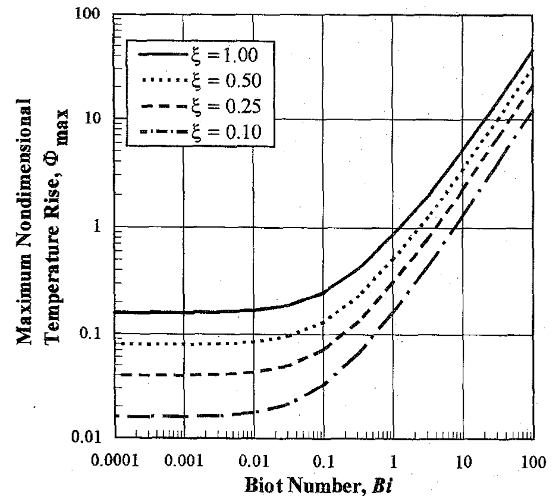

Fig. 7. Maximum nondimensional temperature rise, $\Phi_{\max}$, as a function of Biot number, Bi, and duty cycle, ξ.

($\xi = 1$). For periodically driven heat sources ($\xi < 1$), the heat capacity of the substrate is also a factor in the compromise. However, for the conditions of Fig. 6, heat capacity does not play a significant role in determining the substrate thickness that minimizes temperature.

The depth of the minimum, conversely, is significantly influenced by periodic heating. Figure 6 shows that, under steady-state conditions ($\xi = 1$), the minimum temperature rise is approximately 25% that of a negligibly thin substrate for which $\Phi_{\max} = 1$. However, when the duty cycle is 0.1, the optimal substrate's temperature rise is only 3% that of a very thin substrate. Thus, for periodic heating, a proper choice of substrate thickness is imperative in attaining the smallest possible temperature rise.

The variation of maximum temperature rise with the Biot number, shown in Fig. 7, indicates that, for all Biot numbers examined, there are clear advantages from periodic heating, with increasing benefits as the Biot number is reduced. For very small Biot numbers, conductive resistance is negligible compared to convective resistance, and a uniform substrate temperature could be assumed with reasonable accuracy. In this "lumped capacitance" regime, temperature rise is proportional to the duty cycle; hence, a duty cycle of 0.1 produces a nondimensional temperature rise that is one-tenth of the steady-state value. As the Biot number increases, conductive resistance impedes the flow of heat during off-peak operation, and the benefits of periodic heating are reduced.

In the Fig. 8, the maximum temperature rise is plotted against the Fourier number for several Biot numbers ranging from 0.001–1.0. For a given substrate material and geometry, the Fourier number is directly proportional to the period of the driven heat source. Hence, the abscissa in Fig. 8 may be viewed as a nondimensional cycle period. A lumped capacitance analysis [14] reveals that the factor $Fo \cdot Bi \div l^*$ provides an estimate of the ratio between the cycle period and the overall thermal time constant. For low Bi, relatively high Fo are allowed before $\Phi_{\max}$ increases. As Bi increases, lower Fo must be selected in order to realize the lowest possible $\Phi_{\max}$. As an example, consider a typical package with an aluminum oxide substrate ($a = 0.01$ m, $k = 36$ W/mK, $\alpha = 11.9 \times 10^{-6}$ m^2/s) in mixed air convection ($h = 36$ W/m^2-K), giving $Bi = 0.01$. The results of Fig. 8 suggest that cycle periods up to $p = 84$ s ($Fo = 10$) can be achieved with little temperature rise above the minimum asymptote.

The duty cycle may also be varied in order to reduce the temperature rise. The maximum temperature rise is plotted in Fig. 9 as a function of duty cycle for several power ratios. The figure illustrates that for $0 < \beta < 1$ (i.e., nonzero off-peak heat flux) the temperature asymptotes to a finite steady-state solution as $\xi \rightarrow 0$. As the duty cycle approaches 1, all curves approach the steady-state result. For purely on–off operation ($\beta = 0$), the temperature rise goes to zero as $\xi \rightarrow 0$, resulting in extremely small temperature rises for small duty cycles. The results may also be expressed in terms of the allowable heat flux. For instance, given a maximum temperature rise of 53°C and a heat transfer coefficient of 100 W/m^{2}K, the results of

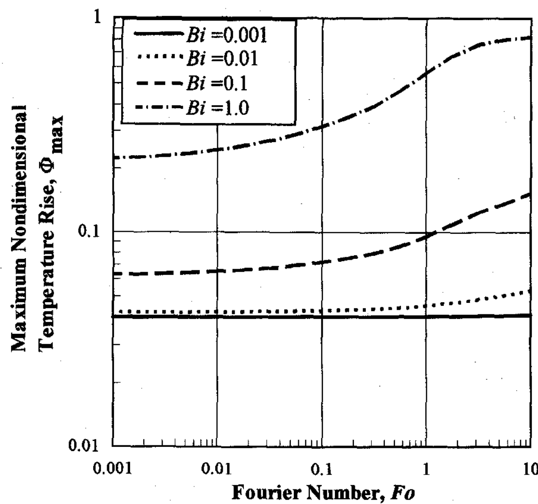

Fig. 8. Maximum nondimensional temperature rise, $\Phi_{\max}$, as a function of Fourier number, Fo, and Biot number, Bi.

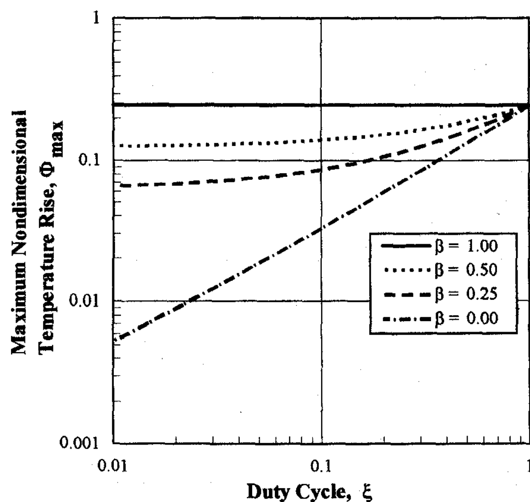

Fig. 9. Maximum nondimensional temperature rise, $\Phi_{\max}$, as a function of duty cycle, ξ, and power ratio, β.

Fig. 9 suggest that a heat flux of $q''_{\max} = 100$ W/cm^2 could be achieved for $\xi = 0.01$ and $\beta = 0$.

IV. Conclusions

Series solutions for the transient response of the common heat source-on-substrate problem are provided for the case of a square-wave heat flux profile. The maximum temperature rise is shown to depend on the substrate thickness, substrate radius, Biot number, Fourier number, duty cycle, and power ratio. The results presented indicate that, with an appropriate choice of parameters, periodic heating can substantially reduce chip temperatures by utilizing the heat capacity of the substrate. In particular, optimal substrate thicknesses exist, and cycle periods up to tens of seconds can be implemented while realizing substantial benefits from periodic heating for the chip-on-substrate geometry under typical packaging conditions.

In the present study, we have attempted to quantify the thermal benefits of periodic heating. Although not considered here, the concept can be extended to substrates with enhanced heat storage materials, such as phase change materials. In addition, other issues such as reliability and electrical implementation must also be considered in greater detail in order to fully assess feasibility and practicality of periodic operation.

Acknowledgment

The authors appreciate discussions with Dr. B. G. Sammakia (IBM, Endicott) and Prof. K. E. Torrance and C.-Y. Li (Cornell University).

References

[1] A. Bar-Cohen, "State-of-the-art and trends in the thermal packaging of electronic equipment," *ASME J. Electron. Packag.*, vol. 114, pp. 257–270, Sept. 1992.

[2] D. Strassberg, "Dynamic power management—μP cooling's future," *EDN*, p. 43, Jan. 20, 1994.

[3] V. Kadambi and N. Abuaf, "Axisymmetric and three-dimensional chip-spreader calculations," in *AIChE Symp. Series*, Seattle, WA, 1983, vol. 79, no. 225, pp. 130–139.

[4] S. K. Hingorani, C. J. Fahrner, D. W. Mackowski, J. S. Goodling, and R. C. Jaeger, "Optimal sizing of planar thermal spreaders," *ASME J. Heat Transfer*, vol. 116, no. 2, pp. 296–301, May 1994.

[5] T. S. Fisher, F. A. Zell, K. K. Sikka, and K. E. Torrance, "Efficient heat transfer approximation for the chip-on-substrate problem with convection," *ASME J. Electron. Packag.*, to be published.

[6] L. M. Buller, "Thermal transients in electronic packages," *IEEE Trans. Comp., Hybrids, Manufact. Technol.*, vol. CHMT-3, no. 4, pp. 588–594, Dec. 1980.

[7] J. W. Sofia, "Analysis of thermal transient data with synthesized dynamic models for semiconductor devices," in *10th IEEE SEMI-THERM Symp.*, 1994, pp. 78–85.

[8] L. P. Cao, J. P. Krusius, T. S. Fisher, and C. T. Avedisian, "Transient energy management strategies for portable systems," in *Proc. 45th ECTC*, 1995, pp. 1161–1165.

[9] B. M. Guenin, "Transient thermal model for the MQUAD® microelectronic package," in *Proc. 10th IEEE SEMI-THERM Symp.*, 1994, pp. 86–95.

[10] J. Lohan and M. Davies, "Transient thermal behavior of a board-mounted 160-lead plastic quad flat pack," in *1994 InterSociety Conf. Thermal Phenomena*, 1994, pp. 108–116.

[11] N. Zommer and D. L. Feucht, "Analytical thermal response of a multiple-layer device under the semi-infinite approximation," *IEEE Trans. Electron Devices*, vol. ED-25, no. 4, pp. 441–448, Apr. 1978.

[12] V. Kadambi and N. Abuaf, "An analysis of the thermal response of power chip packages," *IEEE Trans. Electron Devices*, vol. ED-32, no. 6, pp. 1024–1033, June 1985.

[13] M. I. Flik, B. I. Choi, and K. E. Goodson, "Heat transfer regimes in microstructures," *ASME J. Heat Transfer*, vol. 114, pp. 666–674, 1992.

[14] V. S. Arpaci, *Conduction Heat Transfer*. Reading, MA: Addison-Wesley, 1966, chs. 2, 5, and 6.

Timothy S. Fisher received the B.S. degree from Cornell University, Ithaca, NY, in 1991.

From 1991 to 1993, he worked as a packaging engineer in the Automotive and Industrial Electronics Group of Motorola. He is currently pursuing a doctoral degree in the Sibley School of Mechanical and Aerospace Engineering at Cornell University. His research interests include numerical and experimental studies of coupled solid–fluid systems and transient thermal phenomena in semiconductors.

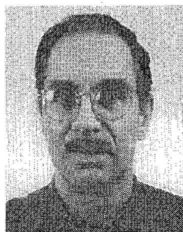

C. Thomas Avedisian received the Ph.D. degree from Princeton University, in 1980.

In 1980, he joined the faculty of Mechanical and Aerospace Engineering at Cornell University, where he is currently a full professor. He was employed at AT&T Bell Laboratories in Holmdel, NJ, in 1974, as a member of the technical staff, and has spent sabbatic leaves at the National Institute of Standards and Technology, and Brown University. His research interests are in the thermal design of electronic packages, and has taught a course on the subject at Cornell. Recent work concerns heat sink design, including heat pipes and fluid jet impingement, for cooling microprocessors and other electronic devices, and using laser techniques for measuring the thermal conductivity of materials.

J. Peter Krusius (M'80–SM'87) received the Ph.D. degree from Helsinki University of Technology, Helsinki, Finland.

After obtaining his Ph.D. degree, he worked as a Research Associate at Dortmund University, Institute of Theoretical Physics, West Germany, as a Docent at the Electron Physics Laboratory, Helsinki University of Technology. He came to the School of Electrical Engineering at Cornell University as a Fulbright Fellow in 1979, where he continued as a Research Associate before becoming an Associate Professor in 1981. In 1987, he became a full Professor at Cornell. He has spent sabbatic leaves at the IBM Research Center, Yorktown Heights, NY, and at the Royal Institute of Technology, Stockholm, Sweden. He is Director of the Joint Services Electronic Program at Cornell University and the Associate Director of the Electronic Packaging Program.